ESAIM: PROCEEDINGS AND SURVEYS, August 2023, Vol. 72, p. 2-18
Philippe Helluy, Jean-Marc Hérard, Nicolas Seguin

STUDY OF RELAXATION PROCESSES IN A TWO-PHASE FLOW MODEL

Jean Bussac[1]

Abstract. This work concerns the analysis of the relaxation processes toward thermodynamical equilibrium arising in a compressible immiscible two-phase flow. Classically the relaxation processes are taken into account through dynamical systems which are coupled to the dynamics of the flow. The present paper compares two types of source terms which are commonly used: a BGK-like system and a mixture entropy gradient type. For both systems, main properties are investigated (agreement with second principle of thermodynamics, existence of solutions, maximum principle,...) and numerical experiments illustrate their asymptotic behaviour.

1. Introduction

This paper enters the framework of the modelling of compressible multiphase flows. Numerous models have been developed in order to depict their dynamics as well as the thermodynamical disequilibrium between the phases [1, 2, 16]. several approaches exist, we focus here on the two-phase modelling. On the one hand, the two-fluid models consider that the two phases evolve with their own velocities, leading to a model composed of two Euler-type systems coupled through nonconservative terms involving so-called interfacial quantities and relaxation source terms [1]. In this paper, we concentrate on the one-velocity approach, so that the disequilibrium only concerns thermal and mechanical exchanges as well as mass transfer between the two phases. Such models, referred as homogeneous models [2, 10, 15, 18], enjoy many pros (compared to two-fluid models), notably a conservative form and thus well defined schock relations. In the homogeneous approach, one can assume that the phases are at thermodynamical equilibrium, leading to the class of Homogeneous Equilibrium Models. In this case, the system corresponds to one Euler system (for the mixture conserved quantities) with a complex closure pressure law $\bar{P}(\tau, e)$ which has to depict the thermodynamical behaviour of the mixture, for a given state of volume τ and internal energy e [4]. Such models are often inoperable because of the complexity of the mixture pressure law. A convenient way to get rid of this complexity is to relax the pressure law by making it depend on additional quantities Y, for instance the fractions of volume α, of mass y and energy z of one of the two phases. Then the pressure law is $P(\tau, e, Y)$ and the system is completed with additional equations on these fractions with source terms $\Gamma(\tau, e, Y)$, which have to depict the relaxation towards the thermodynamical equilibrium Y_{eq}, such that

$$P(\tau, e, Y_{eq}) = \bar{P}(\tau, e).$$

Such models are called Homogeneous Relaxation Models (HRM) and have proved to be relevant alternative to two-fluid models [10]. If there is a consensus on the convective part of HRM models, the derivation of the relaxation source term is still a prominent question. Indeed all the thermodynamical disequilibria are depicted

[1] Université de Nantes, Laboratoire de Mathématiques Jean Leray (LMJL - UMR 6629), F-44000 Nantes, France

Article published online by EDP Sciences and available at https://www.esaim-proc.org or https://doi.org/10.1051/proc/202372002

by the dynamical system

$$\frac{dY}{dt}(t) = \Gamma(\tau, e, Y). \tag{1}$$

Admissible source terms have to fulfill two major constraints:

(1) Second principle of thermodynamics: the source term has to guarantee the growth of the thermodynamical entropy $s(\tau, e, Y)$ of the mixture (and, similarly, the decrease of the mathematical entropy). A sufficient condition in the case of the Homogeneous Relaxation Models is to impose

$$\Gamma(\tau, e, Y) \cdot \nabla_Y s(\tau, e, Y) \geq 0; \tag{2}$$

(2) Asymptotic states: for a given state (τ, e) of the fluid, the source terms have to capture the right thermodynamical equilibrium, that is

$$\lim_{t\to\infty} Y(t) = Y_{eq}. \tag{3}$$

The aim of the present paper is to compare two possible forms of source terms. The first one, recently referred as BGK source term [12], corresponds to a linearization around the equilibrium state Y_{eq}. Its apparition goes back to [2, 7, 14] and is now used in multiphase configurations with complex phasic equation of state (EOS) [11, 19]. The alternative source term corresponds to the gradient form of the mixture entropy, which directly fulfills (2) [18].

In Section 2 the thermodynamics of the two-phase mixture is presented, considering that both phases satisfy a Stiffened Gas law and are immiscible. The thermodynamical equilibrium is defined as the result of the maximization of the mixture entropy and its standard properties are recalled. Section 3 and 4 gather properties of these two choices of source terms, when considering a mixture of two Stiffened Gases. The advantage of this particular equation of state is that it allows to obtain relevant results while keeping a reasonable degree of complexity. In both sections, we investigate the eligibility and consistency of the source terms and list their major features: asymptotic state, trajectories, numerical resolution... Some remarks will be given on the influence of relaxation time scales. In the concluding Section 5, a comparison is proposed.

2. Thermodynamics of an immiscible two-phase mixture

This section concerns the thermodynamical description of the two-phase mixture. We adopt an intensive description, which can be deduced from an extensive one, see [5, 15] for a proper derivation. We consider a fluid of intensive volume τ and internal energy e, composed of two phases that we label $k = 1, 2$. Each phase k is depicted by its phasic intensive volume τ_k and internal energy e_k. Following standard thermodynamics, the phase k is entirely described by an entropy function, which properties are stated in the following paragraph.

Then while investigating the mixture intensive entropy, we characterize the thermodynamical equilibrium. It results from a maximization of the mixture entropy under the constraints of mass conservation, energy conservation and immiscibility of the two phases. These three constraints are expressed in terms of fractions of mass y_k, energy z_k and volume α_k of the phase k, so that the maximization process provides a characterization of the equilibrium vector Y_{eq}. Note that the miscible case is treated in Appendix A.

2.1. Phasic equation of state

We focus here on the intensive description of the phase k: a unit of mass can be described by its specific volume $\tau_k > 0$ and its specific energy $e_k > 0$, using an entropy function $(\tau_k, e_k) \mapsto s_k(\tau_k, e_k)$. By adopting the Gibbs formalism, the entropy function complies with the following differential form

$$T_k \mathrm{d}s_k = \mathrm{d}e_k + P_k \mathrm{d}\tau_k, \tag{4}$$

where the phasic temperature T_k and pressure P_k are defined by

$$\frac{1}{T_k} = \left.\frac{\partial s_k}{\partial e_k}\right|_{\tau_k}, \qquad P_k = T_k \left.\frac{\partial s_k}{\partial \tau_k}\right|_{e_k}. \tag{5}$$

The phasic chemical potential is defined by the relation

$$\mu_k = -T_k s_k + P_k \tau_k + e_k. \tag{6}$$

The phasic entropy functions are supposed to be

- strictly concave function of (τ_k, e_k) on $(\mathbb{R}_*^+)^2$,
- of class C^2, such that $\forall (\tau_k, e_k) \in (\mathbb{R}_*^+)^2,\ T_k(\tau_k, e_k) > 0$.

These standard assumptions derive from hypothesis usually made on the extensive entropies, see [15].

In the sequel, we will focus on a particular choice of phasic equation of state, namely the Stiffened Gas equation. This equation has the advantage of being a quite realistic model while keeping a reasonable degree of complexity in the following analysis.

The phasic entropy function is defined by

$$s_k(\tau_k, e_k) = C_k(\ln(e_k - Q_k - \Pi_k \tau_k) + (\gamma_k - 1)\ln(\tau_k)) + s_k^0, \tag{7}$$

where $C_k > 0$ is the heat capacity, $-\Pi_k$ is the minimal pressure, Q_k is a reference enthalpy, $\gamma_k > 1$ is the adiabatic coefficient and $s_k^0 > 0$ is a reference specific entropy. This is an extension of the perfect gas law [17], which corresponds to the simpler case $\Pi_k = Q_k = 0$.

For further numerical experiments, we focus on parameters given in [19] for a liquid (with index 1) and vapor water (with index 2), which have been determined by an optimization process

Parameters	Phase 1	Phase 2
γ_k	1.39864082368510	1.15442237458290
C_k	$3.19641035947920\times10^3$	$2.91668522329726\times10^3$
Q_k	$-1.24606074764184 \times 10^6$	$1.25942536895827 \times 10^6$
Π_k	$4.79690712132593 \times 10^8$	$-3.24993579473092 \times 10^2$
s_k^0	-34597.52986978335	-33792.18353359583

TABLE 1. Stiffened Gas parameters

2.2. **Mixture entropy function**

Let $w = (\tau, e)$ be the state vector of the two-phase fluid. It is composed of two phases of specific volume τ_k and e_k, such that

$$\tau_k = \frac{\alpha_k}{y_k}\tau, \quad e_k = \frac{z_k}{y_k}e, \tag{8}$$

where $y_k \in [0,1]$ is the mass fraction of the phase k, $\alpha_k \in [0,1]$ the volume fraction and $z_k \in [0,1]$ the energy fraction. The mass and energy conservation impose that

$$\begin{cases} y_1 + y_2 = 1, \\ z_1 + z_2 = 1, \end{cases} \tag{9}$$

while assuming that the two phases are immiscible, the volume constraint is

$$\alpha_1 + \alpha_2 = 1. \tag{10}$$

Note that Appendix A investigates the case of a miscible mixture which corresponds to the constraint $\alpha_1 = \alpha_2 = 1$.

In order to simplify notations, we note $Y = (y, \alpha, z) = (y_1, \alpha_1, z_1)$ such that

$$\begin{cases} y_2 = 1 - y, \\ \alpha_2 = 1 - \alpha, \\ z_2 = 1 - z. \end{cases}$$

The intensive entropy of the mixture is given by

$$s(\tau, e, Y) = y s_1(\frac{\alpha}{y}\tau, \frac{z}{y}e) + (1-y)s_2(\frac{1-\alpha}{1-y}\tau, \frac{1-z}{1-y}e). \tag{11}$$

It is defined on a convex subset of $(\mathbb{R}_+)^2 \times]0;1[^3$. Following [15], in order to capture single phase configuration, namely $Y = (0,0,0)$ (pure vapor) or $Y = (1,1,1)$ (pure liquid), we extend the entropy function on

$$C := (\mathbb{R}_+)^2 \times (]0;1[^3 \cup 0_{\mathbb{R}^3} \cup 1_{\mathbb{R}^3}),$$

with notations $0_{\mathbb{R}^3} = (0,0,0)$ and $1_{\mathbb{R}^3} = (1,1,1)$, by

$$s(\tau, e, Y) := \begin{cases} s_1(\tau, e), & \text{if } Y = 1_{\mathbb{R}^3}, \\ s_2(\tau, e), & \text{if } Y = 0_{\mathbb{R}^3}. \end{cases} \tag{12}$$

The expression (11) can be deduced from the extensive form of the mixture entropy, see [4, 5, 7, 15]. As a consequence, concavity properties result from those of the extensive entropy, namely:

- for a given Y, $(\tau, e) \mapsto s(\tau, e, Y)$ is concave,
- for a given (τ, e), $Y \mapsto s(\tau, e, Y)$ is concave.

In the case of a mixture of two Stiffened Gases, the entropy s is

$$\begin{aligned} s(\tau, e, Y) = {} & y C_1(\ln(\frac{z}{y}e - Q_1 - \Pi_1 \frac{\alpha}{y}\tau) + (\gamma_1 - 1)\ln(\frac{\alpha}{y}\tau)) \\ & + (1-y)C_2(\ln(\frac{1-z}{1-y}e - Q_2 - \Pi_2 \frac{1-\alpha}{1-y}\tau) + (\gamma_2 - 1)\ln(\frac{1-\alpha}{1-y}\tau)). \end{aligned}$$

Definition 2.1. The set of admissible fractions for a given intensive state $w = (\tau, e) \in (\mathbb{R}_*^+)^2$ is

$$C_w = \{Y \in]0;1[^3 \cup 0_{\mathbb{R}^3} \cup 1_{\mathbb{R}^3}, (\tau, e, Y) \in C\}. \tag{13}$$

Proposition 2.2. *For any couple $w = (\tau, e) \in (\mathbb{R}_*^+)^2$, C_w is an open unit cube subset bounded by two planes $\mathcal{P}_1$ and $\mathcal{P}_2$:*

$$C_w = \left\{ (y, \alpha, z) \in]0;1[^3,\ z > \frac{Q_1}{e}y + \frac{\Pi_1 \tau}{e}\alpha,\ (1-z) > \frac{Q_2}{e}(1-y) + \frac{\Pi_2 \tau}{e}(1-\alpha) \right\},$$

where $\mathcal{P}_1 = \{(y, \alpha, z) \in \mathbb{R}^3, z = \frac{Q_1}{e}y + \frac{\Pi_1 \tau}{e}\alpha\}$ and $\mathcal{P}_2 = \{(y, \alpha, z) \in \mathbb{R}^3, (1-z) = \frac{Q_2}{e}(1-y) + \frac{\Pi_2 \tau}{e}(1-\alpha)\}$. Moreover, $0_{\mathbb{R}^3} \in \mathcal{P}_1$ and $1_{\mathbb{R}^3} \in \mathcal{P}_2$.

Figure 1 represents the set of admissible fractions C_w for a given state $(\tau = 0.01, e = 10^7)$ and Stiffened Gas law s_k, $k = 1, 2$, with parameters (1). The planes $\mathcal{P}_1$ and $\mathcal{P}_2$ are represented in red and blue. Observe that the pure states $0_{\mathbb{R}^3}$ and $1_{\mathbb{R}^3}$ belong to the planes $\mathcal{P}_1$ and $\mathcal{P}_2$ respectively. In the case of perfect gases, the plane $\mathcal{P}_1$ (resp. $\mathcal{P}_2$) coincides with the plane $\{z = 0\}$ (resp. $\{z = 1\}$).

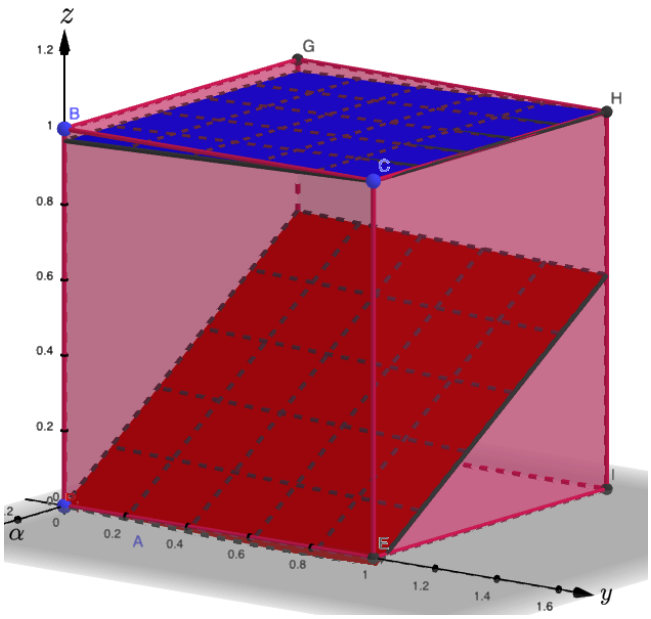

FIGURE 1. Set of admissible fractions C_w for $\tau = 0.01$ and $e = 10^7$ and Stiffened Gas parameters (1). The state $0_{\mathbb{R}^3}$ belongs to the plane $\mathcal{P}_1$ (in red) and the state $1_{\mathbb{R}^3}$ to the plane $\mathcal{P}_2$ (in blue), see Proposition 2.2. In this particular case, one remarks that $E \in C_w$ while $B, C, G, I, J \notin C_w$.

2.3. Thermodynamical equilibrium

The second law of thermodynamics states that for any thermodynamical evolution, the entropy of the mixture cannot decrease and that the equilibrium corresponds to the maximum of the entropy.

Definition 2.3. For a given $w = (\tau, e) \in (\mathbb{R}_*^+)^2$, the equilibrium fraction $Y_{eq} \in C_w$ maximises the mixture entropy $Y \mapsto s(\tau, e, Y)$ on C_w. In other words

$$Y_{eq}(w) = \underset{Y \in C_w}{\arg\max}\, s(\tau, e, Y). \tag{14}$$

The study of this optimization procedure has been the topic of numerous studies, notably for immiscible mixtures of Stiffened Gas law [4, 10, 11, 19].

When the maximum is reached in the interior of the domain C_w, then the equilibrium corresponds to a saturation state [7, 14].

Proposition 2.4. *When the maximum of the entropy is reached in the interior of the set of constraints C_w, it is characterized by the equality of phasic pressures, temperatures and chemical potentials:*

$$\begin{cases} P_1(\tau_1, e_1) = P_2(\tau_2, e_2), \\ T_1(\tau_1, e_1) = T_2(\tau_2, e_2), \\ \mu_1(\tau_1, e_1) = \mu_2(\tau_2, e_2). \end{cases} \tag{15}$$

Let us point out major features.

- When the maximum is reached in the interior of C_w, it is not sure that Y_{eq} is well defined. Indeed, the entropy function is only concave (and not strictly concave) on C_w, so that Y_{eq} is not necessarily uniquely defined, see Remark 2.5.

- The continuous extension of the mixture entropy guarantees that Y_{eq} can take the values $0_{\mathbb{R}^3}$ or $1_{\mathbb{R}^3}$, that correspond to the single phase equilibria.
- The difficulty of the computation of Y_{eq} directly depends of the chosen equations of state. For a mixture of two Stiffened Gases, it consists of a algebraic problem, given in [10], but for more complex EOS such as Noble-Able-Stiffened Gases (NASG) or NASG-Chemkin laws [19], non explicit changes of variables lead to tedious computations, which become even worse when considering additional phases, see [13,19].
- In [9], the authors affirm that the equilibrium is a single phase state in most cases. It would be interesting to verify this on a statistical study by choosing a relevant domain for (τ, e).

Remark 2.5. Attempts of proof concerning this strict concavity of the mixture entropy have been provided for instance in [13]. They rely on the study of the concavity of the extensive mixture.

The idea is to show, for a given extensive state $W = (M, V, E)$ (with mass M, volume V and energy E), that the extensive mixture entropy S is a strictly concave function when restricted on the set $\mathcal{H}(M)$ of the states whose total mass is equal to M. If this property is true, it follows the strict concavity of the intensive entropy.

In order to prove the strict concavity of S on $\mathcal{H}(M)$, the idea is to show that the degeneracy manifold of S, $\ker \nabla^2_W S(W)$ coincide with $\mathrm{Vect}(W)$, that is to say:

$$\forall W,\ \ker \nabla^2_W S(W) = \mathrm{Vect}(W). \tag{16}$$

If so, then the restriction of S on $\mathcal{H}(M)$ is strictly concave since $\mathcal{H}(M) \cap \ker \nabla^2_W S(W) = \{W\}$. However, only the inclusion $\mathrm{Vect}(W) \subset \ker \nabla^2_W S(W)$ is shown [15]. One remarks that $\ker \nabla^2_W S(W)$ is a vectorial subset in the 6-dimensional space in the case of a two-phase flow. The second inclusion seems difficult to show.

Since the strict concavity property of the mixture entropy s is crucial to model a physically relevant system, a brief numerical study has been done on the sign of $\nabla_Y s(\tau, e, Y)$. No fraction such as $\nabla_Y s(\tau, e, Y) = 0$ have been found for the case presented on Figure 1, for 10^9 values tested in $]0;1[^3$.

3. BGK-like source term

This first type of source terms corresponds to a BGK linearized form for two-phase mixture. It has been introduced in the homogeneous literature, first in the two-phase case [2, 7, 10, 14] and more recently in the multiphase context [13, 19].

For a given state $(\tau, e, Y) \in C$, supposing $Y \mapsto s(\tau, e, Y)$ is *strictly* concave, there exists a unique equilibrium fraction state Y_{eq} which maximises the entropy s, where Y_{eq} only depends of (τ, e), see Definition 2.3.

Definition 3.1. For any state $(\tau, e, Y) \in C$, we define

$$\Gamma_1(\tau, e, Y) = \frac{1}{\boldsymbol{\lambda}}(Y_{eq}(\tau, e) - Y), \tag{17}$$

where $\boldsymbol{\lambda} = (\lambda_1, \lambda_2, \lambda_3)$ is a time scales vector and $\frac{1}{\boldsymbol{\lambda}} Y$ means the term by term product.

This definition involves time scales $\boldsymbol{\lambda}$ which generally depend on time and are distinct. They correspond respectively to the mass transfer, the mechanical and thermal relaxation times.

Eligibility and Consistency. *Let $\lambda \in \mathbb{R}^*_+$ be such that $\lambda_1 = \lambda_2 = \lambda_3 = \lambda$. For any given state $(\tau, e) \in (\mathbb{R}^+_*)^2$, assume that the entropy function $(\tau, e, Y) \mapsto s(\tau, e, Y)$ is strictly concave with respect to Y. Then, the source terms Γ_1 complies with the entropy growth criterion (2). Moreover, the stationary states of the dynamical system (1)-(17) coincide with the possible thermodynamical equilibria of Definition 2.3.*

Proof. It is obvious that the stationary states of the source term Γ_1 are vector Y_{eq} of Definition 2.3. It remains to check the entropy growth. Let $(\tau, e, Y) \in C$ be a given state. It holds

$$\begin{aligned}
\Gamma_1(Y) \cdot \nabla_Y s(\tau, e, Y) &= (\frac{1}{\boldsymbol{\lambda}}(Y_{eq} - Y)) \cdot \nabla_Y s(\tau, e, Y) \\
&= (\frac{1}{\lambda}(Y_{eq} - Y)) \cdot \nabla_Y s(\tau, e, Y) \\
&= \frac{1}{\lambda}(Y_{eq} - Y) \cdot \nabla_Y s(\tau, e, Y) \\
&\geq \frac{1}{\lambda}(s(\tau, e, Y_{eq}) - s(\tau, e, Y)) \\
&\geq 0,
\end{aligned}$$

thanks to the concavity of $Y \mapsto s(\tau, e, Y)$. □

Note that invoking the concavity argument requires to consider a unique relaxation parameter λ. Recently a modification of BGK-like source terms which allows distinct time scales has been introduced in [12].

Proposition 3.2. *Let $(\tau, e, Y_0) \in C$ be an initial state. The Cauchy problem*

$$\begin{cases} \frac{dY}{dt}(t) = \Gamma_1(\tau, e, Y(t)), \quad t > 0 \\ Y(0) = Y_0 \end{cases}, \tag{18}$$

admits a global solution Y given by

$$\forall t \geq 0, \ Y(t) = e^{-\boldsymbol{\Lambda}(t)}(e^{\boldsymbol{\Lambda}(0)}Y(0) + Y_{eq}\int_0^t \boldsymbol{\lambda}(s)e^{\boldsymbol{\Lambda}(s)}\mathrm{d}s), \tag{19}$$

where $\boldsymbol{\Lambda}$ is a primitive of $1/\boldsymbol{\lambda}$. In the case of a constant in time relaxation parameter $\boldsymbol{\lambda}$, it holds

$$\forall t \geq 0, \ Y(t) = e^{-t/\boldsymbol{\lambda}}Y(0) + (1 - e^{-t/\boldsymbol{\lambda}})Y_{eq}. \tag{20}$$

This last expression can be interpreted as a barycenter of the initial state $Y(0)$ and the equilibrium state Y_{eq}. Trajectories of the solutions are exponential towards equilibrium fractions. Figure 2 illustrates this behaviour for a mixture of two Stiffened Gases with parameters (1). One observes the evolution in time of the fractions $Y(t)$ for an initial state $Y(0) = (0.5, 0.5, 0.5)$, with specific volume $\tau = 5.5.10^{-3}$ and internal energy $e = 10^8$. The time scale is constant in time and set to $\boldsymbol{\lambda} = 1$. The equilibrium fractions, represented by the dotted lines, are reached at time $t = 6$s. Another important point is that the time when the asymptotic state is reached does not depend on the initial state of the fluid.

One major advantage of the BGK-like source term is that it can be explicitly integrated. However it requires to determine the equilibrium state Y_{eq} for every considered state $(\tau, e, Y) \in C$, that is to say solve the maximization problem (14). For two-phase mixture, and especially Stiffened Gas law, the maximization can be done explicitly [10]. But when more complex EoS are considered and the number of phases increases, the maximization has to be realized with an appropriate optimization algorithm: one is proposed in the case of three Stiffened Gases in [3], another one uses a Broyden method for a mixture of two stiffened gases plus a NASG-Chemkin law in [19]. When coupled with the fluid dynamics, for instance through a time splitting approach, this maximization procedure has to be performed in each control volume and at each time step, leading to a complex resolution and higher CPU costs, see [3].

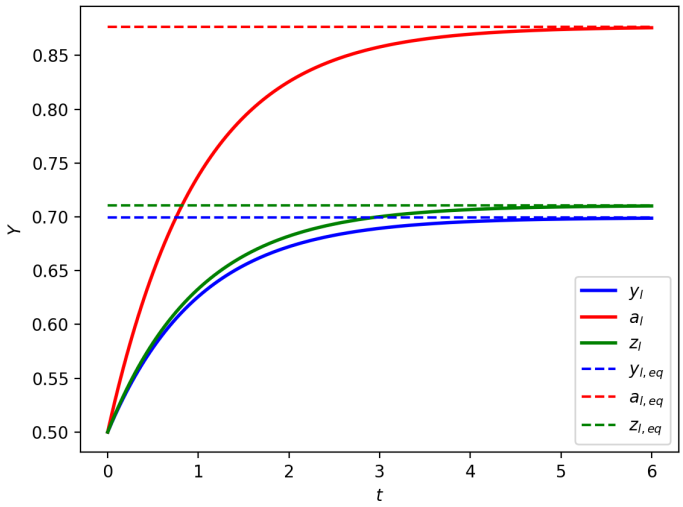

FIGURE 2. Trajectories of the system Γ_1 for the data $Y(0) = (0.5, 0.5, 0.5)$, $\tau = 5.5.10^{-3}$, $e = 10^8$ and $\boldsymbol{\lambda} = 1$. EOS parameters are given in Table (1). The equilibrium state is represented by the dotted lines asymptotes.

4. Entropy gradient source term

The second type of source terms corresponds to the entropy gradient such that it directly satisfies the eligibility condition (2).

Definition 4.1. For all $(\tau, e, Y) \in C$, the source term Γ_2 reads

$$\Gamma_2(\tau, e, Y) = \frac{1}{\boldsymbol{\lambda}} Y(1-Y) \nabla_Y s(\tau, e, Y), \tag{21}$$

with $\boldsymbol{\lambda} = (\lambda_1, \lambda_2, \lambda_3)$ relaxation parameters. Using the mixture entropy definition (11) and the phasic potentials (5)-(6), Γ_2 rewrites

$$\Gamma_2 = \begin{pmatrix} \frac{y(1-y)}{\lambda_1}(\frac{\mu_2}{T_2} - \frac{\mu_1}{T_1}) \\ \frac{\alpha(1-\alpha)}{\lambda_2}\tau(\frac{P_1}{T_1} - \frac{P_2}{T_2}) \\ \frac{z(1-z)}{\lambda_3}e(\frac{1}{T_1} - \frac{1}{T_2}) \end{pmatrix}.$$

In the case of a mixture of two Stiffened Gases, the definition domain of Γ_2 is C_w, represented in Figure 1. The source term Γ_2 corresponds to the entropy gradient times $Y(1-Y)$ (understood as term by term product). This modification is mandatory for numerical purposes. Indeed the set of definition of the mixture entropy $Y \mapsto s(Y)$ is C_w which is included in $]0;1[^3$. Thus a solution Y of the dynamical system $Y'(t) = \nabla_Y s(\tau, e, Y)$ is such that $Y(t) \in]0;1[^3$, for all $t > 0$ (unless the dynamical system is not defined). However in numerical applications, this maximum principle is not guaranteed, even for smaller time steps, as illustrated in Figure 3-left. It corresponds to a mixture of two stiffened gases with parameters (1) depicted by the dynamical system $Y'(t) = \nabla_Y s(\tau, e, Y)$ with initial state $Y(0) = (0.5, 0.5, 0.5)$, $\tau = 8.10^{-4}$, $e = 10^8$ and $\boldsymbol{\lambda} = 1$. One observes that the volume fraction becomes nonpositive at time $t < 0.0025$s. The correction term $Y(1-Y)$ ensures the maximum principle as illustrated in Figure 3-right. Of course, this correction term modifies the trajectories, in particular the single phase equilibrium state seems to be reached at a longer time in the Figure 3 example.

Every approximated solutions of the dynamical system (21) have been obtained with Adams-Bashforth plus backward differenciation formula types algorithms, using Python Scipy library.

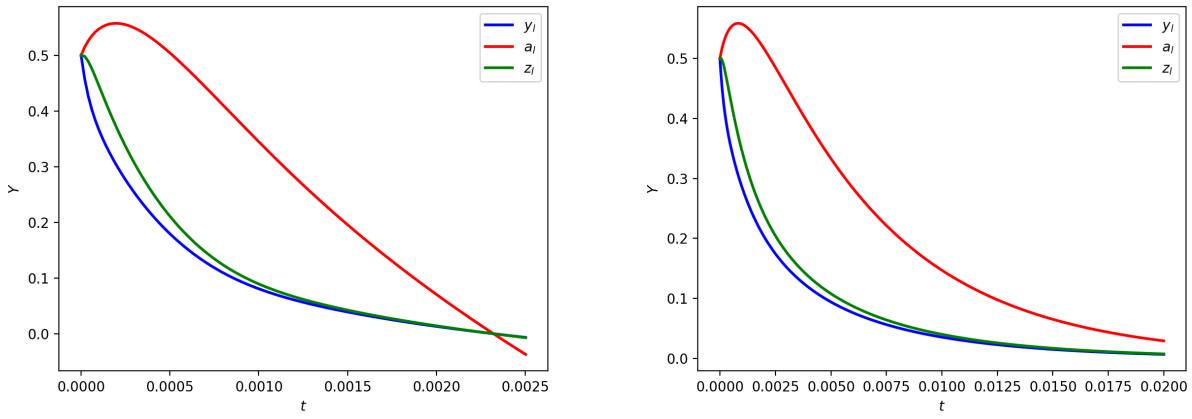

(A) Trajectories for $\Gamma_2 = \nabla_Y s$.

(B) Trajectories for $\Gamma_2 = Y(1-Y)\nabla_Y s$.

FIGURE 3. Comparison of the trajectories of the solutions of $\dot{Y} = \nabla_Y s(\tau, e, Y)$ (left) and $\dot{Y} = Y(1-Y)\nabla_Y s(\tau, e, Y)$ (right) for a mixture of Stiffened Gases with parameters (1). The initial data is $Y(0) = (0.5, 0.5, 0.5)$, with $\tau = 8.10^{-4}$, $e = 10^8$ and $\boldsymbol{\lambda} = 1$.

Remark 4.2. The source term Γ_2 involves the difference of phasic pressures which acts on the volume fraction equation. Such an expression is rather classical. It can be found in the two-fluid literature, for instance in Baer-Nunziato like model [1] and the derivation of such mechanical transfer term is now well understood [6].

Eligibility and Consistency. *Assume that there exists* $\lambda_0 \in \mathbb{R}_+^*$ *such that* $\forall t \geq 0,\ \forall k = 1,2,3,\ \lambda_k(t) < \lambda_0$. *For any given state* $(\tau, e) \in (\mathbb{R}_*^+)^2$, *the source term* Γ_2 *complies with the entropy growth criterion* (2).

Proof. Let us define $\zeta = \inf_k \left(\frac{1}{\lambda_k} Y_k(1-Y_k)\right)$. It holds

$$\begin{aligned}
\Gamma_2(Y) \cdot \nabla_Y s(\tau, e, Y) &= \frac{1}{\boldsymbol{\lambda}} Y(1-Y)\nabla_Y s \cdot \nabla_Y s \\
&= \sum_{k=1}^{3} \frac{1}{\lambda_k} Y_k(1-Y_k)(\partial_{Y_k} s)^2 \\
&\geq \zeta \sum_{k=1}^{3} (\partial_{Y_k} s)^2 \\
&\geq \zeta ||\nabla_Y s||_2^2 \\
&\geq 0,
\end{aligned}$$

which concludes the proof. □

Unlike the previous BGK-like source terms, solving exactly the system is out of reach. However existence en uniqueness of local solution to Cauchy problem is guaranteed by the Cauchy-Lipschitz theorem.

Proposition 4.3. *Consider* $(\tau, e) \in (\mathbb{R}_*^+)^2$. *For all* $Y_0 \in (\mathbb{R}_*^+)^3$ *such that* $(\tau, e, Y_0) \in C$, *there exists an unique maximal solution* $(I, Y) \in \mathbb{R}_+ \times]0;1[^3$, *with* $Y : I \to]0;1[^3$, *of the system* (1)-(21).

The following purpose is to ensure that the stationary states of the dynamical system (1)-(21), namely vector $\bar{Y}$ such that $\Gamma_2(\bar{Y}) = 0$, correspond to physically relevant thermodynamical equilibria of the two-phase mixture, in the sense of (3).

For a given state $(\tau, e) \in (\mathbb{R}_*^+)^2$, if $\bar{Y} \in]0;1[^3$, then $\Gamma_2(\bar{Y}) = 0$ implies that $\nabla_Y s(\tau, e, \bar{Y}) = 0$. Hence $\bar{Y}$ is such that (15) holds and the thermodynamical equilibrium is a stationary state.

On the other hand, since Γ_2 is not defined on the border of the cube $[0,1]^3$, one cannot determine if single phase states $\bar{Y} = 0_{\mathbb{R}^3}$ or $\bar{Y} = 1_{\mathbb{R}^3}$ are stationary states of the dynamical system and if these states are attractive (using standard arguments like the jacobian linearization). In a similar way, $(1,0,0)$ could be a stationary state of the dynamical system, even if it has no physical sense. The following result states that trajectories Y cannot reach the border of the cube $[0,1]^3$ in the case of a mixture of two Stiffened Gases with parameters (1).

Proposition 4.4 (Exclusion of the border)**.** *Let $(\tau, e) \in (\mathbb{R}_*^+)^2$ be a given state. For any initial data $Y(0) \in]0,1[^3$, a solution $Y(t)$ of the system (1)-(21) cannot converge towards an asymptotic state belonging to the following sets:*

- *faces:* $\{y = 0\}$, $\{y = 1\}$, $\{\alpha = 0\}$, $\{\alpha = 1\}$,
- *edges:* $\{y = 0, \alpha = 0\}$, $\{y = 1, \alpha = 1\}$, $\{y = 0, \alpha = 1\}$, $\{y = 1, \alpha = 0\}$, $\{y = 0, z = 1\}$, $\{y = 1, z = 0\}$, $\{\alpha = 0, z = 1\}$, $\{\alpha = 1, z = 0\}$,
- *corners:* $(1;0;0)$, $(0;1;0)$, $(1;0;1)$, $(0;1;1)$.

Proof. The proof relies on vector field argument. We study the limits of Γ_2 in the neighbourhood of the different considered sets, by supposing that it is defined in these areas, that depends on the thermodynamical parameters.

- $\forall (\alpha, z) \in]0;1[^2$, $\lim\limits_{y \to 0} \Gamma_2(Y) = \left(0, k_1, k_2\right)^\top$ with $k_1 \in \mathbb{R}$ and $k_2 \in \mathbb{R}_*^-$. Since $k_2 \neq 0$, there is no possible equilibrium around the face $\{y = 0\}$. This case is illustrated on Figure 4 for several initial fractions $Y(0) \in]0,1[^3$ (blue dots) with trajectories converging towards an asymptotic state (red triangle) corresponding to a saturation state. Observe that, since $k_2 < 0$, the curves are decreasing functions of α in the neighbourhood of the face $\{y = 0\}$.
- $\forall (\alpha, z) \in]0;1[^2$, $\lim\limits_{y \to 1} \Gamma_2(Y) = \left(0, k_1, k_2\right)^\top$, $k_1 \in \mathbb{R}$, $k_2 \in \mathbb{R}_+^*$,
- $\forall (y, z) \in]0;1[^2$, $\lim\limits_{\alpha \to 0} \Gamma_2(Y) = \left(-\infty, k_1, k_2\right)^\top$, $k_1 \in \mathbb{R}_+^*$, $k_2 \in \mathbb{R}$,
- $\forall (y, z) \in]0;1[^2$, $\lim\limits_{\alpha \to 1} \Gamma_2(Y) = \left(+\infty, k_1, k_2\right)^\top$, $k_1 \in \mathbb{R}_-^*$, $k_2 \in \mathbb{R}$.

Concerning the planes $\{z = 0\}$, $\{z = 1\}$, there could exist couples (y, α) such that the following k_1, k_2 are both null. Indeed, we have

$$\forall (y, \alpha) \in]0;1[^2, \ \lim_{z \to 0,1} \Gamma_2(Y) = \left(k_1, k_2, 0\right), \ (k_1, k_2) \in \mathbb{R}^2,$$

and so rigorously, we cannot conclude.

Let us introduce the notation $\lim f = *$ which means that f does not admit a limit or it cannot be determined. As edges are concerned, it holds:

- $\forall z \in]0;1[$, $\lim\limits_{y,\alpha \to 0} \Gamma_2(Y) = \left(*, 0, k_1\right)^\top$, $k_1 \in \mathbb{R}_-^*$,
- $\forall z \in]0;1[$, $\lim\limits_{y,\alpha \to 1} \Gamma_2(Y) = \left(*, 0, k_1\right)^\top$, $k_1 \in \mathbb{R}_+^*$,
- $\forall y \in]0;1[$, $\lim\limits_{\alpha,z \to 0} \Gamma_2(Y) = \left(-\infty, k_1, 0\right)^\top$, $k_1 \in \mathbb{R}_+^*$,
- $\forall y \in]0;1[$, $\lim\limits_{\alpha,z \to 1} \Gamma_2(Y) = \left(+\infty, k_1, 0\right)^\top$, $k_1 \in \mathbb{R}_-^*$,
- $\forall z \in]0;1[$, $\lim\limits_{y \to 0,\ \alpha \to 1} \Gamma_2(Y) = \left(*, k_1, k_2\right)^\top$, $(k_1, k_2) \in (\mathbb{R}_-^*)^2$,
- $\forall z \in]0;1[$, $\lim\limits_{y \to 1,\ \alpha \to 0} \Gamma_2(Y) = \left(*, k_1, k_2\right)^\top$, $(k_1, k_2) \in (\mathbb{R}_+^*)^2$,
- $\forall y \in]0;1[$, $\lim\limits_{\alpha \to 0,\ z \to 1} \Gamma_2(Y) = \left(-\infty, k_1, k_2\right)^\top$, $(k_1, k_2) \in \mathbb{R}^2$,

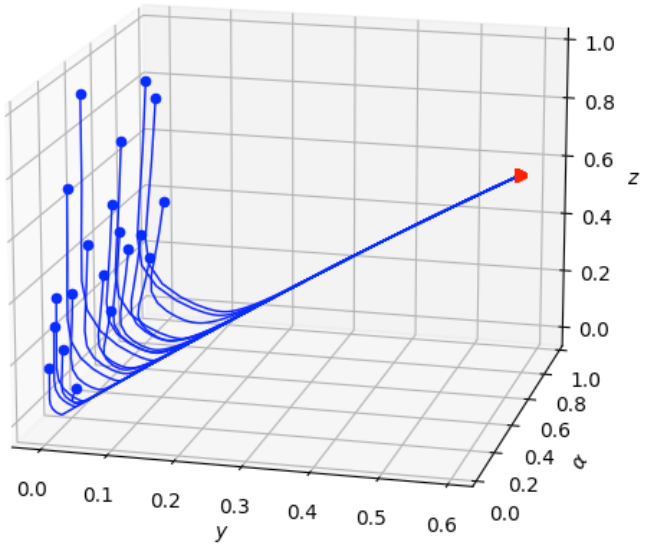

FIGURE 4. Trajectories of the system (1)-(21) with different initial fractions $Y(0) = (1.10^{-10}, \alpha, z)$ where (α, z) is randomly chosen in $]0;1[^2$. Initial states are represented by blue dots. Thermodynamical parameters are given in Table (1), $\tau = 5.10^{-2}$, $e = 10^8$ and $\lambda = 1$. The initial data $Y(0) \in]0,1[^3$ is represented by a blue dot and the corresponding asymptotic state is represented in red.

- $\forall y \in]0;1[, \lim_{\alpha\to 1,\ z\to 0} \Gamma_2(Y) = \big(+\infty, k_1, k_2\big)^\top,\ (k_1,k_2) \in \mathbb{R}^2.$

Four edges remain problematic because of undetermined limits.

Finally, we can exclude four among the six corners:

- $\lim_{y\to 1,\ \alpha,z\to 0} \Gamma_2(Y) = \big(*, k_1, 0\big)^\top,\ k_1 \in \mathbb{R}_+^*,$
- $\lim_{y\to 0,\ \alpha,z\to 1} \Gamma_2(Y) = \big(*, k_1, 0\big)^\top,\ k_1 \in \mathbb{R}_-^*,$
- $\lim_{\alpha\to 1,\ y,z\to 0} \Gamma_2(Y) = \big(*, k_1, 0\big)^\top,\ k_1 \in \mathbb{R}_-^*,$
- $\lim_{\alpha\to 0,\ y,z\to 1} \Gamma_2(Y) = \big(*, k_1, 0\big)^\top,\ k_1 \in \mathbb{R}_+^*,.$

For the two remaining corners $(1,1,0)$ and $(0,0,1)$, two components of Γ_2 do not admit a limit or the limit is undetermined. □

We emphasize that these arguments do not apply for the two corners $(1,1,0)$ and $(0,0,1)$ and the two faces $\{z=0\}$and $\{z=1\}$. Some improvements may be done while considering specific parameters Q_k and π_k. For instance, the realistic parameters (1) exclude some of these last sets as one can see on Figure 1, since Γ_2 is not defined on these areas. In these cases, we could investigate what happens on the planes, where the same phenomena can occur. The same kind of arguments hold since being in the neighbourhood of a plane induce limits towards $\pm\infty$ for some components of Γ_2.

When considering a perfect gas mixture, the proof holds true and the corners $(1,1,0)$ and $(0,0,1)$ and the two faces $\{z=0\}$ and $\{z=1\}$ are not reachable as well.

In practical simulations, we did not find any case of trajectories with asymptotic states belonging to these sets. Some trajectories are plotted in Figure 5 in the case of an immiscible mixture of two Stiffened Gases with parameters (1), using standard Python semi-implicit algorithm that are sufficient for a two Stiffened

Gas mixture. All the curves correspond to a solution of the dynamical system (1)-(21) with the initial data $Y(0) = (0.5, 0.5, 0.5)$ with $\boldsymbol{\lambda} = 1$. The internal energy is $e = 10^8$ and different specific volumes are considered. The green curve correspond to $\tau = 1.10^{-3}$ and asymptotically converges towards the state $0_{\mathbb{R}^3}$, that is to the presence of the phase 2 only. The blue curve corresponds to the case $\tau = 1.10^{-2}$ and converges towards the single phase asymptotic state $1_{\mathbb{R}^3}$ (only the phase 1 is present). The red curve is obtained with $\tau = 5.5.10^{-3}$ and corresponds to a saturation state $Y_{eq} \in]0, 1[^3$ satisfying (2.4).

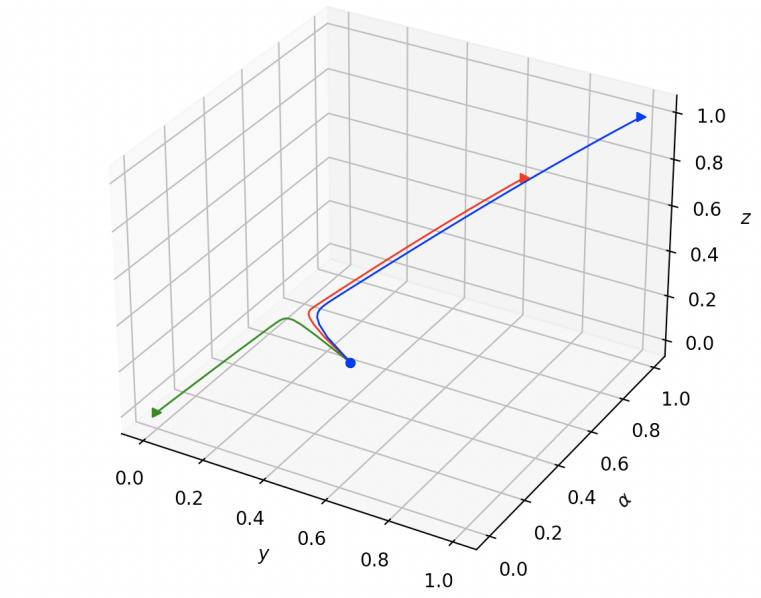

FIGURE 5. Examples of trajectories of the dynamical system Γ_2 with initial data $Y(0) = (0.5, 0.5, 0.5)$ and $e = 10^8$. The green curve is obtained with $\tau = 1.10^{-3}$ and converges towards the single phase state $0_{\mathbb{R}^3}$. The blue curve corresponds to $\tau = 1.10^{-2}$ and converges towards the single phase state $1_{\mathbb{R}^3}$. The red curve with $\tau = 5.5.10^{-3}$ converges to a saturation state in the interior of the cube.

Figure 6 illustrates possible asymptotic states of the dynamical system (1)-(21). For a given internal energy $e = 10^8$, each trajectory corresponds to a given initial state $(\tau, e, Y(0))$, where $Y(0)$ and τ are determined randomly respectively in $]0, 1[^3$ and in $]5.10^{-4}; 1.10^{-2}[$. The initial fraction $Y(0)$ is represented by a blue dot and the asymptotic states with final time $t = 0.1$ are plotted in red. One observes that the asymptotic states are distributed in the interior of the cube and the corners $0_{\mathbb{R}^3}$ and $1_{\mathbb{R}^3}$ appear to be accumulation points.

5. Concluding comparison of the source terms

The BGK-like source terms provide very simple solutions, as soon as the equilibrium state Y_{eq} is known for a given state $(\tau, e) \in (\mathbb{R}_*^+)^2$. The trajectories are of exponential type. In particular the time to return to equilibrium is always the same, no matter is the initial data. As the source term Γ_2 is concerned, we cannot give an explicit form of the solutions. In the general case, its trajectories are far more complex, notably non monotone, and the return to equilibrium directly depends on the initial state.

Figure 7 presents trajectories for a two stiffened gas mixture with parameters (1) . They are obtained, for both source terms, for a state $\tau = 5.5.10^{-3}$, $e = 10^8$ with a relaxation time $\boldsymbol{\lambda} = 1$. The same initial state $Y(0) = (0.5, 0.5, 0.5)$ is considered. One observes that the trajectories for the BGK-like system have the expected exponential behaviour. On the contrary, trajectories of the entropy gradient source term are non

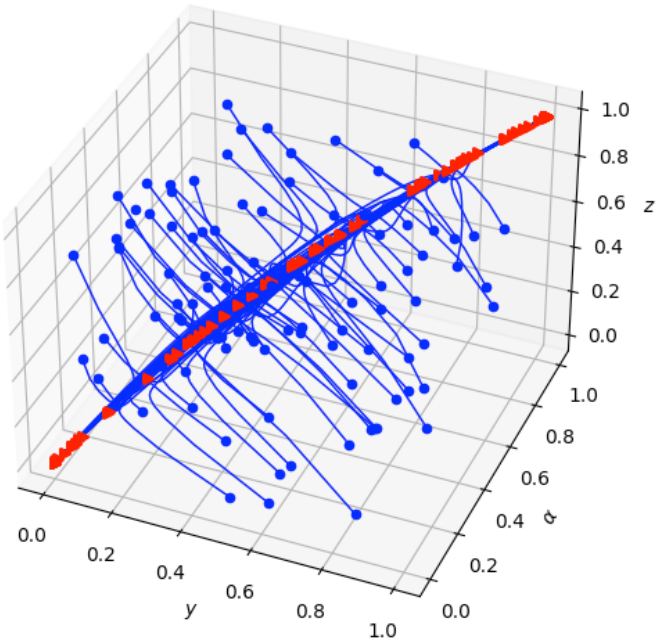

FIGURE 6. Trajectories of the dynamical system Γ_2 with $e = 10^8$ and $\boldsymbol{\lambda} = 1$. Each trajectory correspond to a randomly chosen pair $(Y(0), \tau) \in]0, 1[^3 \times]5.10^{-4}; 1.10^{-2}[$ where the initial data $Y(0)$ is represented by a blue dot. The corresponding asymptotic states are represented in red.

monotone. An interesting point is the time when the asymptotic state is reached: the source term Γ_2 achieves the thermodynamical equilibrium state faster than the BGK-like source term.

To finish a comparison in terms of numerical complexity is mandatory. The BGK-like source term requires to compute the equilibrium fractions Y_{eq} for any state (τ, e). When complex EoS are used, or if we consider more phases, optimization algorithm have to be implemented, see [3, 11, 19]. When coupled with the fluid dynamics, such algorithms are very CPU consuming since they are called in every cell at every time step.

Such complexity could be avoided using the source term Γ_2. Of course, when considering complex phasic EoS or a larger number of phases, such source term can be stiff but semi-implicit or high-order explicit time integration method can be used and provide expected asymptotic states.

Finally, the entropy gradient source term allows to easily consider with different relaxation times for the mechanical, thermal exchange or the mass transfer. This is not the case for the BGK-like source term which requires the maximization of the mixture entropy with a common relaxation time, even if some recent improvements have been done on this topic [12].

Acknowledgments

This work has received the financial support from the ANR MoHyCon and the CNRS project Needs M2SIR. Part of the work has benefited from fruitful discussions with Mrs Hélène Mathis from LMJL, Nantes and Mr Hérard from EDF Lab Chatou. The author would like to thank the reviewer for his detailed feedback.

A. MISCIBLE MIXTURE

The volumic description is more adapted to a miscible mixture [8]. A unit of volume of the phase $k = 1, 2$ is fully described by its volumic mass $\rho_k = 1/\tau_k > 0$ and its volumic energy $\epsilon_k = \rho_k e_k$, using a volumic entropy

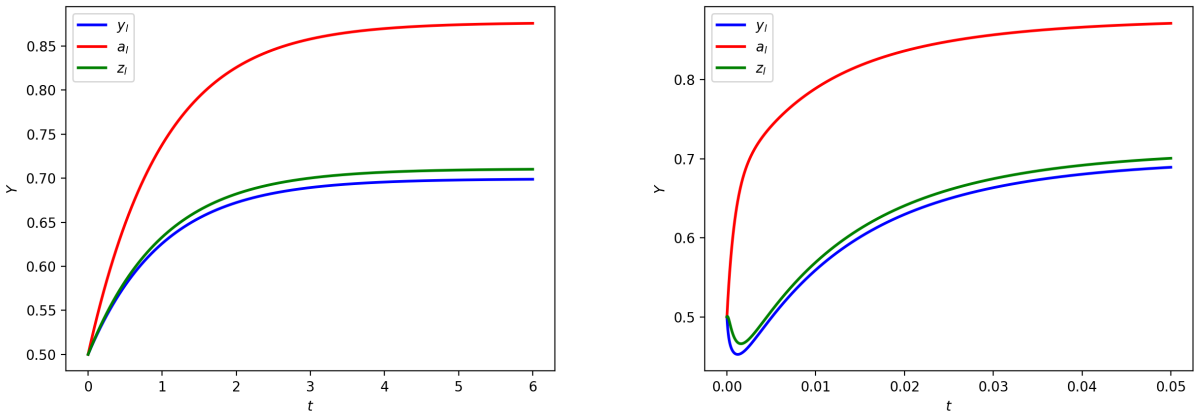

(A) Trajectories for Γ_1

(B) Trajectories for Γ_2

FIGURE 7. Comparison of the trajectories of models Γ_1 and Γ_2 for the same initial data $Y(0) = (0.5, 0.5, 0.5)$, $\tau = 5.5.10^{-3}$, $e = 10^8$, $\boldsymbol{\lambda} = 1$. While Γ_1's trajectories are increasing exponential curves, Γ_2's are not monotone. For the source term Γ_2, the asymptotic state is reached at time $t = 0.05$s, and approximatively at time $t = 3.5$s for the source term Γ_1. Asymptotic states are the same.

function $(\rho_k, \epsilon_k) \mapsto \tilde{s}_k(\rho_k, \epsilon_k)$. Note that $\tilde{s}_k = \rho_k s_k$. We have the following relations, see [5] for a more complete description

$$T_k \mathrm{d}\tilde{s}_k = \mathrm{d}\epsilon_k - \mu_k \mathrm{d}\rho_k, \tag{22}$$

with the definitions

$$\frac{1}{T_k} = \left.\frac{\partial \tilde{s}_k}{\partial \epsilon_k}\right|_{\rho_k}, \qquad \mu_k = -T_k \left.\frac{\partial \tilde{s}_k}{\partial \rho_k}\right|_{\epsilon_k}, \tag{23}$$

and the pressure verifies

$$P_k = T_k \tilde{s}_k + \rho_k \mu_k - \epsilon_k. \tag{24}$$

Similarly to the specific case, we suppose that the phasic volumic entropies are strictly concave functions of their variables.

In the miscible case, both phases share the same volume, which gives equal volume fractions $\alpha_1 = \alpha_2 = 1$ Consequently, we only have two constraints, namely mass and energy conservation

$$\begin{cases} y_1 + y_2 = 1 \\ z_1 + z_2 = 1 \end{cases}. \tag{25}$$

Hence the description in the miscible case requires one variable less than in the immiscible one. A unit of volume is described by $\tilde{w} = (\rho, \epsilon)$, where ρ is the volumic mass and ϵ is the volumic energy. We note in the following $\tilde{Y} = (y, z) = (y_1, z_1)$ the fraction of mass and energy of the phase 1.

Finally, the volumic mixture entropy $\tilde{s}$ is given by

$$\tilde{s}(\rho, \epsilon, \tilde{Y}) = \tilde{s}_1(y\rho, z\epsilon) + \tilde{s}_2((1-y)\rho, (1-z)\epsilon), \tag{26}$$

whose definition domain $\tilde{C}$ is a convex subset of $(\mathbb{R}_+)^2 \times (]0;1[^2 \cup 0_{\mathbb{R}^2} \cup 1_{\mathbb{R}^2})$, see [5] for a derivation from the extensive setting. Since $\tilde{s}$ is the sum and a composition of strictly concave and affine functions, we have the following results

- for a given $\tilde{Y}$, $(\tau, e) \mapsto \tilde{s}(\tau, e, \tilde{Y})$ is strictly concave,
- for a given (τ, e), $\tilde{Y} \mapsto \tilde{s}(\tau, e, \tilde{Y})$ is strictly concave.

When considering a miscible mixture of two Stiffened Gases, the definition domain $\tilde{C}_{\tilde{w}}$ of $\tilde{Y} \mapsto \tilde{s}(\rho, \epsilon, \tilde{Y})$ is a subset of $]0;1[^2$ bounded by two lines

$$\tilde{C}_{\tilde{w}} = \{(y,z) \in]0;1[^2,\ z > \frac{Q_1\rho}{\epsilon}y + \frac{\Pi_1}{\epsilon},\ z < -\frac{Q_2\rho}{\epsilon}y - \frac{\Pi_2}{\epsilon} + 1\}. \tag{27}$$

Following the Section 2.3, we can characterize the thermodynamical equilibrium of a miscible two-phase mixture. We emphasize two main differences: firstly, the entropy maximization is done in the two-dimensional space, and secondly, the equilibrium fractions are well defined thanks to the strict concavity of $\tilde{Y} \mapsto \tilde{s}(\tau, e, \tilde{Y})$.

Definition A.1. For a given $\tilde{w} = (\rho, \epsilon) \in (\mathbb{R}_*^+)^2$, we define $\tilde{Y}_{eq} \in \tilde{C}_{\tilde{w}}$ the equilibrium fraction which maximises the mixture entropy $\tilde{Y} \mapsto \tilde{s}(\tau, e, \tilde{Y})$ on $\tilde{C}_{\tilde{w}}$:

$$\tilde{Y}_{eq}(\tilde{w}) = \underset{\tilde{Y} \in \tilde{C}_w}{\arg\max}\, \tilde{s}(\rho, \epsilon, \tilde{Y}), \tag{28}$$

where $\tilde{C}_{\tilde{w}} = \{\tilde{Y} \in]0;1[^2 \cup 0_{\mathbb{R}^2} \cup 1_{\mathbb{R}^2}, (\rho, \epsilon, \tilde{Y}) \in \tilde{C}\}$.

The properties of Section 2.3 can be stated for $\tilde{C}_{\tilde{w}}$ and $\tilde{Y}_{eq}$, the main difference is the two-dimensional space framework.

When the maximum is reached in the interior of the domain C_w, it is characterized by the equality of phasic temperatures and chemical potential, plus the Dalton's law on phasic pressures [5, 8] :

$$\begin{cases} T_1(\rho_1, \epsilon_1) = T_2(\rho_2, \epsilon_2) \\ \mu_1(\rho_1, \epsilon_1) = \mu_2(\rho_2, \epsilon_2) \\ P(\rho, \epsilon, \tilde{Y}) = P_1(\rho_1, \epsilon_1) + P_2(\rho_2, \epsilon_2) \end{cases}. \tag{29}$$

We now define the miscible counterparts of the dynamical systems Γ_1 and Γ_2.

For the BGK-like source terms, the main difference with the immiscible case is that the equilibrium state Y_{eq} is always well defined since the mixture entropy is striclty concave. The properties of the system are the same: existence, trajectory behaviour.

The entropy gradient source terms can be defined in the same way that in the immiscible case, but once again in the two-dimensional space. It reads

$$\tilde{\Gamma}_2(\rho, \epsilon, \tilde{Y}) = \frac{1}{\boldsymbol{\lambda}} \tilde{Y}(1 - \tilde{Y}) \nabla_{\tilde{Y}} \tilde{s}(\rho, \epsilon, \tilde{Y}), \tag{30}$$

with $\boldsymbol{\lambda} = (\lambda_1, \lambda_2)$ relaxation parameters. Using the mixture entropy definition (26) and the phasic potentials (23)-(24), $\tilde{\Gamma}_2$ rewrites

$$\tilde{\Gamma}_2 = \begin{pmatrix} \frac{y(1-y)}{\lambda_1} \rho (\frac{\mu_2}{T_2} - \frac{\mu_1}{T_1}) \\ \frac{\alpha(1-\alpha)}{\lambda_2} \epsilon (\frac{1}{T_1} - \frac{1}{T_2}) \end{pmatrix}.$$

Let us give similar properties of Proposition 4.4. It consists of studying the trajectories around the border of the square $]0;1[^2$. As in the immiscible case, the proof relies on vector field argument. The asymptotic behaviour of $\tilde{\Gamma}_2$ is investigated in the neighbourhood of the edges of the square.

Proposition A.2. *Let $(\rho, \epsilon) \in (\mathbb{R}_*^+)^2$ be a given state. For any initial data $Y(0) \in]0;1[^2$, a solution Y of the system (1)-(30) cannot converge towards an asymptotic state belonging to the edges $\{y = 0\}$ or $\{y = 1\}$.*

One remarks that this property can be stated for both edges $\{z = 0\}$ and $\{z = 1\}$ by choosing thermodynamical parameters and using the constraints (27).

Some trajectories are represented on Figure 8 in the (y, z) plane. They correspond to data $(Y(0), \rho) \in]0, 1[^2 \times]10^1; 10^3[$ chosen randomly, while $\epsilon = 10^{13}$. The initial states are represented by blue dots. The red triangles are asymptotic states and correspond to saturation states or single phase equilibria (top-right triangles).

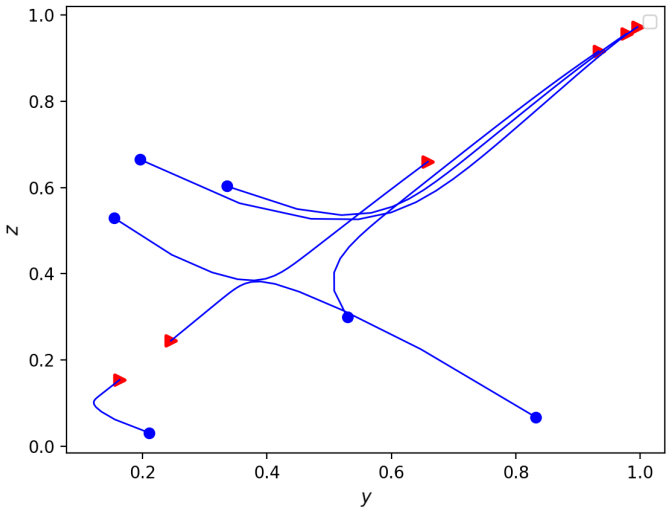

FIGURE 8. Trajectories of the dynamical system $\tilde{\Gamma}_2$ with $\epsilon = 10^{13}$ for a miscible mixture. Each trajectory correspond to a randomly chosen pair $(Y(0), \rho) \in]0, 1[^2 \times]10^1; 10^3[$ where the initial data $Y(0)$ is represented by a blue dot. The corresponding asymptotic states are represented in red. Thermodynamical parameters are given in Table (1) and $\boldsymbol{\lambda} = 1$.

REFERENCES

[1] M. R. Baer and J. W. Nunziato. A two-phase mixture theory for the deflagration-to-detonation transition (ddt) in reactive granular materials. *International journal of multiphase flow*, 12(6):861–889, 1986.

[2] T. Barberon and P. Helluy. Finite volume simulation of cavitating flows. *Computers and Fluids*, 34(7):832–858, 2005. URL: https://hal.archives-ouvertes.fr/hal-00139597.

[3] J. Bussac and H. Mathis. Simulation of an Homogeneous Relaxation Model for a three-phase mixture with miscible phases. Preprint, February 2022. URL: https://hal.archives-ouvertes.fr/hal-03566970.

[4] G. Faccanoni. Étude d'un modèle fin de changement de phase liquide-vapeur. Contribution à l'étude de la crise d'ébullition. November 2008. Thèse en cotutelle entre l'École Polytechnique et l'Università di Trento (Italie). URL: https://pastel.archives-ouvertes.fr/tel-00363460.

[5] G. Faccanoni and H. Mathis. Admissible Equations of State for Immiscible and Miscible Mixtures. *ESAIM: Proceedings and Surveys*, 66:1–21, October 2019. URL: https://hal-univ-tln.archives-ouvertes.fr/hal-01913810, doi:10.1051/proc/201966001.

[6] S. Gavrilyuk. The structure of pressure relaxation terms: the one-velocity case. Technical report, EDF, H-I83-2014-0276-EN, 2014.

[7] P. Helluy. *Simulation numérique des écoulements multiphasiques : de la théorie aux applications*. Habilitation à diriger des recherches, Université du Sud Toulon Var, 2005. URL: https://tel.archives-ouvertes.fr/tel-00657839.

[8] P. Helluy and H. Mathis. Pressure laws and fast Legendre transform. *Math. Models Methods Appl. Sci.*, 21(4):745–775, 2011. URL: http://dx.doi.org/10.1142/S0218202511005209, doi:10.1142/S0218202511005209.

[9] P. Helluy and N. Seguin. Relaxation models of phase transition flows. *ESAIM: Mathematical Modelling and Numerical Analysis*, 40(2):331–352, 2006. URL: https://hal.archives-ouvertes.fr/hal-00139607.

[10] O. Hurisse. Application of an homogeneous model to simulate the heating of two-phase flows. *International Journal on Finite Volumes*, 11, May 2014. URL: https://hal.archives-ouvertes.fr/hal-01114808.
[11] O. Hurisse. Numerical simulations of steady and unsteady two-phase flows using a homogeneous model. *Computers and Fluids*, 152, July 2017. URL: https://hal.archives-ouvertes.fr/hal-01489039.
[12] O. Hurisse. BGK source terms for out-of-equilibrium two-phase flow models. September 2021. URL: https://hal.archives-ouvertes.fr/hal-03330954.
[13] O. Hurisse and L. Quibel. A homogeneous model for compressible three-phase flows involving heat and mass transfer. *ESAIM: Proceedings and Surveys*, 2019. URL: https://hal.archives-ouvertes.fr/hal-01976903.
[14] S. Jaouen. Etude mathématique et numérique de stabilité pour des modeles hydrodynamiques avec transition de phase. 2001.
[15] J. Jung. Schémas numériques adaptés aux accélérateurs multicoeurs pour les écoulements bifluides. (2013STRAD034), October 2013. URL: https://tel.archives-ouvertes.fr/tel-00876159.
[16] A. K. Kapila, R. Menikoff, J. B. Bdzil, S. F. Son, and D. Stewart. Two-phase modeling of deflagration-to-detonation transition in granular materials: Reduced equations. *Physics of fluids*, 13(10):3002–3024, 2001.
[17] O. Le Métayer, J. Massoni, and R. Saurel. Elaboration des lois d'etat d'un liquide et de sa vapeur pour les modeles d'ecoulements diphasiques. *International Journal of Thermal Sciences*, 43, 2004.
[18] H. Mathis. A thermodynamically consistent model of a liquid-vapor fluid with a gas. *ESAIM: Mathematical Modelling and Numerical Analysis*, 53(1):63–84, 2019.
[19] L. Quibel. Simulation of water-vapor two-phase flows with non-condensable gas. September 2020. URL: https://tel.archives-ouvertes.fr/tel-02941486.